Transactions of the Materials Research Society of Japan 26 [3] 1033-1036 (2001)

NOVEL FUNCTIONAL MAGNETIC OXIDE ARTIFICIAL LATTICES IN STRONGLY CORRELATED ELECTRON SYSTEM

Hidekazu Tanaka, T. Kanki, H. Katsu, J. Zhang, Y. Yamamoto, H. Tabata, T. Kawai

The Institute of Scientific and Industrial Research, Osaka University : 8-1 Mihogaoka, Ibaraki, Osaka 567-0047 Japan.
FAX: 06-6875-2440 , e-mail: h-tanaka@sanken.osaka-u.ac.jp

The magneto-electrical properties of metal oxides with strongly correlated electrons are very sensitive to their carrier concentration, electron transfer, and localized spin states. By integrating these characteristics in artificial lattices, it is possible to control numerous functions through the freedom of degree of the spin, charge, and lattice. We have created novel functional magnetic oxide heterostructures in order to apply them to sensitive and multi-functional devices that respond to a variety of external fields, especially light. In (La,Sr)MnO/$SrTiO_3$ heterojunction, we found that increase of resistivity and decrease of metal-to-insulator transition temperature with the illumination of light of the wavelength less-than-400nm and additional photo-induced metal-insulator transition is observed below 100K with decease of magnetization. This behavior can be explained by photo-electron injection from photo-excited $SrTiO_3$ to (La,Sr)MnO_3 layer. In addition, we found that the strained (La,Ba)MnO_3 thin film shows higher T_C and very large magnetoresistance (50% at 0.8T) at room temperature in spite of relatively small amount of carrier by change of 3d orbital state.

Key words : Transition Metal Oxide, Functional heterojunction Magnetoresistance, Photo-induced Magnetism

1. INTRODUCTION

Materials with strongly correlated electrons exhibit a rich variety of magnetic and electrical properties due to the strong interactions among localized spins, conductive electrons, and lattices. Perovskite-type manganites like (La,A)MnO_3 (A=Ca, Sr, Ba, Pb, *etc*) have been attracting much interest due to showing colossal magnetoresistance (CMR) phenomena [1]. Moreover, the ($La_{1-x}A_x$)MnO_3 compound exhibits a rich variety of electronic and magnetic properties depending on the carrier concentration of x. Actually, the parent compound, $LaMnO_3$, is an antiferromagnetic insulator, whereas the hole doped (p-type) ($La_{1-x}Sr_x$)MnO_3 with composition $0.175<x<0.6$ are ferromagnetic metals with a metal-insulator transition at wide rage of Curie temperatures (T_C) from 250K to 380K [2]. This feature is explained by double exchange interaction through e_g electrons as proposed by Zener [3]. Changing the carrier concentration by external field, we can expect to control both the magnetic and electrical properties dynamically and drastically in this strongly correlated electron system. This is of greater advantage than that of conventional semiconductors.

Formation of p-n junction is an effective approach for reversible modulation of carrier concentration by electric field or light as widely used in the technique of semiconductor devices. Perovskite $SrTiO_3$ is a standard substrate for the deposition of functional perovskite compounds and an insulator with a bandgap of 3.2eV which can generate photo-carriers by being irradiated with ultraviolet light. We report photo-carrier injection effect in the ferromagnetic- ($La_{1-x}Sr_x$)MnO_3/photoactive-$SrTiO_3$ perovskite heterostructure and demonstrate dynamical light control of both magnetic and electrical transport properties of ($La_{1-x}Sr_x$)MnO_3 based on the photo-carrier injection mechanism [4]. In addition, we demonstrate enhancement of CMR at room temperature in strained epitaxial $La_{0.8}Ba_{0.2}MnO_3$ thin film. Usually, it is well known that tensile strain decrease T_C with decrease of transfer integral in (La,Sr)MnO_3 and (La,Ca)MnO_3. T_C of $La_{0.8}Ba_{0.2}MnO_3$ epitaxial thin film is remarkably increasing from 270 K in the bulk to above room temperature with extremely large magnetoresistance of 48 % at 0.8 T at room temperature through the tensile strain [5]. This anomalous strain effect in $La_{0.8}Ba_{0.2}MnO_3$ thin film should be explained by not only transfer integral but also degree of freedom on orbital. We also exhibit new phase diagram of the ($La_{1-x}Ba_x$)MnO_3 strained thin film which is good candidate for room temperature operation of novel functional devices based on the carrier modulation.

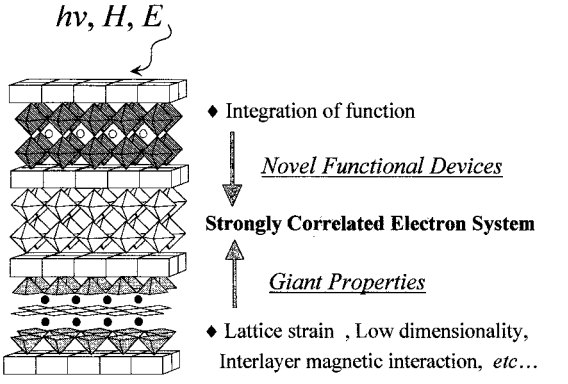

Fig.1 Schematic illustration of function harmonized artificial lattices.

2. EXPERIMETAL

We have fabricated (La,M)MnO_3 (M=Sr or Ba) thin films on $SrTiO_3$ (STO) (100) single crystals by laser ablation technique (ArF excimer laser). The detail has been reported earlier [4, 5]. The STO single crystal, an insulator whose bandgap is 3.2eV, is used for carrier generation layer in this experiment. X-ray diffraction measurement confirmed that the films have c-axis orientation. To evaluate the physical properties of the films, we used a standard four-point probe method in the measurement of temperature dependence of transport property (R-T) and a SQUID magnetometer in the measurement of temperature dependence of magnetization (M-T). The light source is a xenon lamp. The light intensity is about 30mW/mm^{-2} for the R-T measurement and 1mW/ mm^{-2} for the M-T measurement. A sharp cut off filter which cuts the light less than certain wavelength was used in the wavelength dependence measurement.

3. RESULTS AND DISCUSSION

3-1. Photo-control of Magnetism in (La,Sr)MnO_3 /$SrTiO_3$ Functional Heteojunction

Fig. 2 (a) shows temperature dependence of resistivity in a $(La_{0.8}Sr_{0.2})MnO_3$ film (300Å) on a $SrTiO_3$ single crystal substrate (LSMO/STO heterojunction) . The LSMO film underwent metal-to-insulator transition at the Curie Temperature (T_c) of 240K without light irradiation. Under white light irradiation, T_c goes down by 10K to 230K and resistivity increases in the whole temperature range. Remarkably, the resistivity curve jumps up drastically around 100K, and gradually increases below 100K with decreasing temperature, i.e. a semiconductive conduction with a negative $d\rho/dT$ induced by light. To elucidate the origin of this photo-induced metal-to-semiconductor transition, the reference experiments have been done to investigate electrical transport properties in a sintered bulk LSMO alone and a STO single crystal alone under dark and light irradiation, respectively. As for the bulk LSMO, no change was observed with light irradiation. As for $SrTiO_3$, it is noteworthy that resistivity drops sharply to less than 30[Ωcm] around 100K under light irradiation [4], which is the same temperature of resistivity anomaly appearance in the LSMO/STO heterostructure. These phenomena occur only when the sample is irradiated with the lights of wavelength of less-than-400nm corresponding to the bandgap of STO (3.2eV), suggesting that photo induced carriers in the STO substrate is injected into the LSMO layer through interface and change the resistivity. Since the $La_{0.8}Sr_{0.2}MnO_3/SrTiO_3$ hetero-junction exhibits increase of the resistivity around 100K only in heterostructure, the electrical property of LSMO itself must be changed through light irradiation effect.

Since spin and charge are strongly correlated in the double exchange type ferromagnetic (La,Sr)MnO_3, photo-carrier injection effect in the heterojunction is expected to control not only electric transport property but also magnetic property. We have measured the magnetization of LSMO (T_C=150K)/STO heterostructure with irradiation as shown in Fig. 2 (b). As a result, magnetization of LSMO layer decreased below 100K with light having less-than-400nm wavelength. $La_{1-x}Sr_xMnO_3$ whose T_c is less than 230K (hole concentration x being less than 0.15) decreases its magnetization value with decreasing its hole concentration [6]. It is obviously reduced by photo-carriers excited beyond the band gap of STO.

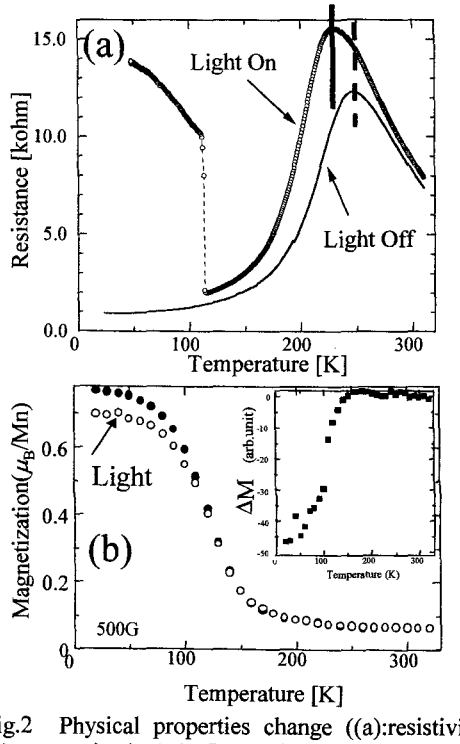

Fig.2 Physical properties change ((a):resistivity, (b) magnetization) in LSMO/STO hetero-junction by light

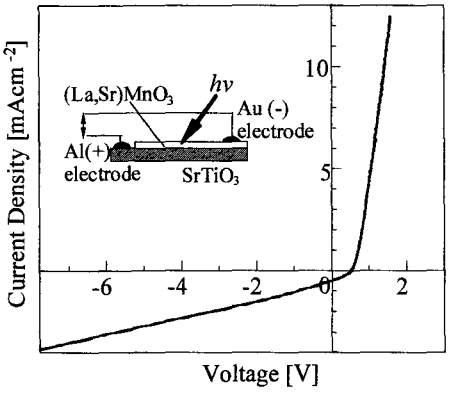

Fig.3 I-V curve of LSMO/STO heterostructure along the perpendicular direction measured at 30K. The inset shows schematic illustration of I-V measurement.

To confirm this carrier injection mechanism, we should observe electrons to be injected from STO to LSMO when the heterojunction is irradiated with light. In this measurement, gold and aluminum electrodes were used on LSMO and STO, respectively, to get ohmic contacts. We have constructed the circuit shown in Fig.3 to investigate the current along perpendicular direction to the interface of LSMO/STO heterostructure at 30K. Due to high resistivity of STO, electric current has not been detected without light irradiation. With irradiation, photo-carrier is generated in STO, so that we are able to detect the current as shown in Fig.3 . We have observed the photovoltage of 500mV by irradiation. This result indicates that electrons generated by photon are injected from STO layer to LSMO layer through the interface at zero bias. Actually, photo current flows at zero bias voltage from LSMO to STO. Without any bias voltage between the heterostructure, electrons are injected into LSMO from STO by light. From these results, the change of electric property in LSMO with light irradiation is explained by reduction of effective carrier concentration (holes for LSMO) due to photo-electrons from STO. In short, the metal phase of LSMO changes into insulative one due to photo-electrons transformed from STO generated by light.

According to the phase diagram of $(La_{1-x}Sr_x)MnO_3$ versus hole concentration [2], reduction of hole concentration weakens ferromagnetic double exchange interaction in LSMO, leading to the increase of resistivity and decrease of T_c. In addition, the anomalous jump of resistivity in LSMO layer with light is obviously related with increase of photoconduction in STO below 100K. The increase of photoconduction strongly suggests that carrier injection efficiency to LSMO layer in the heterostructure increases below 100K. It is considered that this increase of photoconduction in STO originates from its structural phase transition at 105K, changing the electronic structure in STO [4]. As a result, ferromagnetic -metallic (FM) phase of LSMO transformed into ferromagnetic - insulator (FI)

one by the injection of large amount of photo-carrier, that is in accordance with the phase diagram as shown in Fig. 4. We can construct the physical picture that photo-carriers generated in STO substrate is injected to LSMO layer and effective hole concentration in LSMO decreased, leading to change the physical property *via* weakened ferromagnetic double exchange interaction. Therefore, the reduction of magnetization by light can be achieved by photo-carrier (electron) injection from STO layer to LSMO layer same as electrical transport property.

Consequently, we have achieved control of both magnetic and electrical properties of LSMO with light through oxide interfaces.

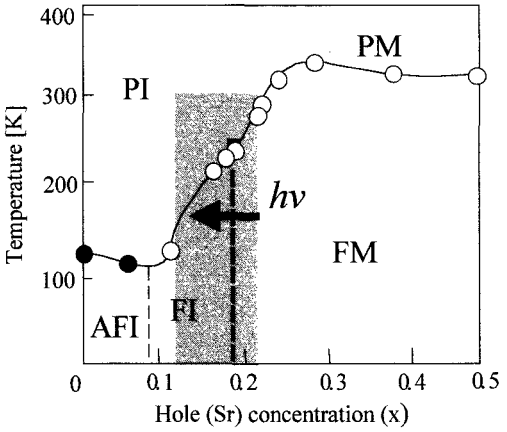

Fig.4 The relationship between photo-control of physical properties and carrier concentration in (La,Sr)MnO_3.

3.-2 Enhancement of Ferromagnetism with Magnetoresistance at Room temperature.

For application of magnetoresistive device or the novel photo-magnetic device mentioned above, it is important that giant properties emerge at room temperature. We have noted relatively high T_C (over room temperature) of (La,Ba)MnO_3 system in spite of small amount of carrier due wide band width, so we have investigate .the change of physical properties when it is deposited on the very important substrate of $SrTiO_3$.

Figs 5(a) and (b) show temperature dependence of magnetization and resistivity of the $(La_{0.8}Ba_{0.2})MnO_3$ films, respectively. T_C of the bulk and the 3900 Å thickness film is almost similar. However, the T_C of the 1000Å, 650Å and 400Å films are much higher (298K - 320K) than that of the bulk. Fig. 5(c) shows temperature dependence of the MR ratio under the magnetic field of 8000 Oe for the bulk and the films with various thickness. The films exhibit higher MR ratio (33% at 320K for 400 Å thickness, 43% at 307K for 650 Å, 45% at 298K for 1000 Å, 48% at 267K for 1300 Å and 47% at 267K for 3900 Å) than that of the bulk (21% at 270K). Although the films with more than 1300Å thickness and bulk material have the same transition temperature (270K), the films exhibit larger MR ratio than bulk material. The metal-insulator transition temperature and maximum value of magnetoresistance strongly depend on film thickness. As a possible reason for this increase of T_C, strain effects with substrate may be considered. Lattice constants are 3.905 Å for $SrTiO_3$ and 3.894 Å for $La_{0.8}Ba_{0.2}MnO_3$ respectively, and lattice mismatch is estimated as -0.28% (tensile strain). Thinner films are more expanded along in-plain direction by substrate so

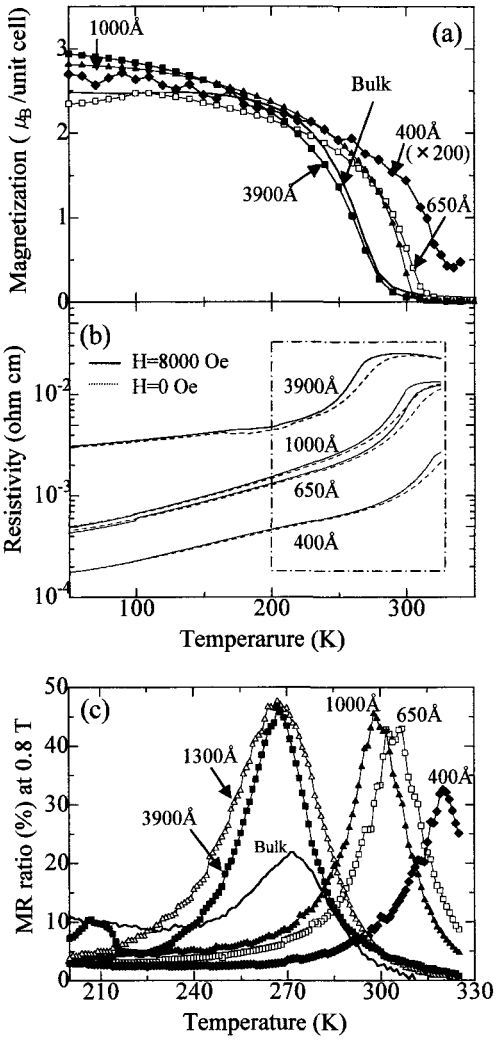

Fig.5 Temperature dependence of (a) magnetization, (b) resistivity and (c) magnetoresistance (H=8000[Oe]) in $(La_{0.8}Ba_{0.2})MnO_3$ thin films with various thickness. MR ratio is defined as MR=(R(0T)-R(0.8T))/R(0.8T)×100[%]

that the degree of crystal field splitting is changed. The energy level of dx^2-y^2 orbital along in-plain direction becomes more stable than that of $d3z^2$-r^2 orbital inducing the increase of conductive electron along in-plain direction that leads to the increase of T_C. Remarkably, the film of 1000 Å thickness exhibits very large magnetoresistance of 48% at 8000[Oe] at room temperature (298K). This MR value at room temperature is very large in comparison with other magnetoresistive oxides [4].

3.-3 New Phase Diagram of the Strained $(La_{1-x}Ba_x)MnO_3$ Films

We have also investigated filing ratio (x) dependence of magnetism in the $(La_{1-x}Ba_x)MnO_3$ deposited on $SrTiO_3$ substrate. By changing x from 0.05 to 0.33, lattice mismatch is systematically changed from -0.76 (tensile) to 0.15 (compressive) to $SrTiO_3$. Furthermore, different electron correlation effect from (La,Sr)MnO_3 system is expected due to larger bandwidth than that of (La,Sr)MnO_3.

For the bulk LBMO with x=0.1, 0.2, 0.3 and 0.33, T_C are 185 K, 280 K, 340 K and 345 K, respectively. Compared with the bulk LBMO, LBMO thin films show

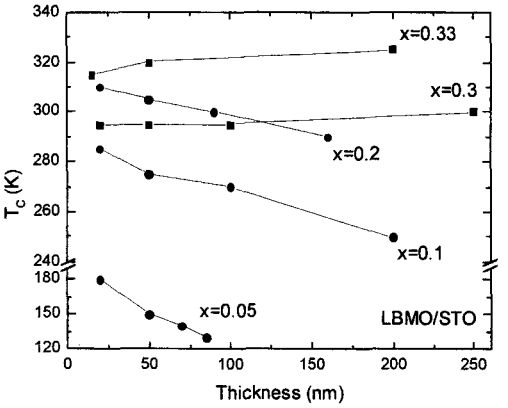

Fig. 6 T_C of LBMO/STO thin films as function of thickness.

much different results. The thickness dependence of T_C for LBMO films is shown in Fig. 6. In the tensile strain region (x=0.05, 0.1 and 0.2), with thickness decreasing, T_C increasing gradually. In the compressive strain range, for the x=0.3 and 0.33 films, T_C is almost thickness independent, and only increases slightly with thickness, which is consistent with the small value of the compressive strains in these doping levels. Although the similar lattice parameters of LBMO and STO prevent us from investigating the thickness dependence of lattice parameters for LBMO thin films with x≥0.1, we observed the out-plane lattice parameter *c* increasing with thickness for x=0.05 thin films, indicating the relaxation of the in-plane tensile strain. With thickness increasing, the lattices of thin films tend to relax, and the strain effect is weakened, resulting in T_C retrieving to the bulk value. The solid relationship between strain relaxation and T_C changing confirms that it is reasonable to attribute the anomalous magnetic properties of LBMO thin films to the strain effect. The enhancement of ferromagnetism by tensile strain in low doping levels is very significant, and room-temperature ferromagnetism was observed in the x=0.1 thin film with thickness of 20 nm, whose T_C is 285 K.

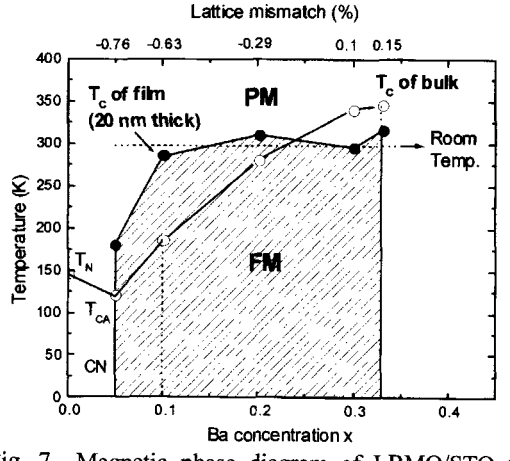

Fig. 7 Magnetic phase diagram of LBMO/STO thin films with thickness 200 Å, as well as that of LBMO bulk compounds as comparison. The lattice mismatches between LBMO and STO are also shown in top axis. FM, PM and CN denote ferromagnetic, paramagnetic, spin canting, respectively

Based on our results, the magnetic phase diagram of LBMO thin films was obtained and shown in Fig. 7. T_C of bulk LBMO is also plotted as a comparison, and the lattice mismatch between bulk LBMO and STO is listed in the top axis. The shadowy region is the ferromagnetic state of LBMO thin films with thickness of 20 nm. It is obviously shown in this phase diagram that ferromagnetism is suppressed by compressive strain and enhanced by tensile strain. Especially, the ferromagnetism around room temperature is obtained for the first time in CMR material with such a low doping level as x=0.1. In addition, we also observed large room temperature CMR effect in x=0.1 thin film (53% at 0.8 T).

4. TOWARD NOVEL FUNCTIONAL HETERO-JUNCTION MADE OF MAGNETORESISTVE OXIDE WITH ROOM TEMPATURE OPERATION.

We believe that this result will open up a "Strongly Correlated Electron Engineering" unifying band gap engineering and Mott transition in strongly correlated electron system as shown in Fig. 8. Toward room temperature operation, LBMO thin film is promising candidate material in this "Strongly Correlated Electron Devices". Due to the small amount of carriers in this thin film, we can expect large changes of its magnetic and transport properties at room temperature by introducing slight fluctuation in the carrier density. Based on this advantage, some new strongly correlated electronic devices can be developed, such as photosensitive magnetic oxide *p-n* junction, and field effect transistor (FET) at room temperature. Photocarrier control of magneto-transport properties has been observed in (La, Sr)MnO_3/STO heterostructure [4], and may be more prominent even at room temperature for LBMO based device. Also in the Ferroelectric FET such as (La,Ca)MnO_3/PZT heterostructure [7], $La_{0.9}Ba_{0.1}MnO_3$ will give better performance can be achieved in that FET device.

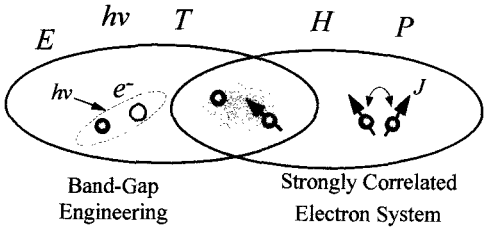

Fig. 8 Concept of "Strongly Correlated Electron Engineering" unifying band gap engineering and Mott transition in strongly correlated electron system..

REFERENCES

[1] S. Jin, T. H. Tiefel, M. McCormark, R. A. Fastnacht, R. Ramesh and L. H. Chen, Science. **264**, 413 (1994)
[2] A.Urashiba, Y.Moritomo, T. Arima, A. Asamitsu, G .Kida, and Y. Tokura, Phys.Rev.**B 51**, 14103 (1995)
[3] C. Zener ,Phys. Rev. **82** 403 (1951)
[4] H. Katsu, H. Tanaka, and T. Kawai, Appl. Phys. Lett. **76**, 3245 (2000)
[5] T. Kanki, H. Tanaka, and T. Kawai, Solid State Commun. **114**, 267 (2000).
[6] G. H. Jonker, Physica. **22**, 707 (1956)
[7] S. Mathews, R. Ramesh, T. Venkatesan, and J. Benedetto, Science **276**, 238 (1997)

(Received December 8, 2000; Accepted December 25, 2000)